

Supporting Information

Tunable Emission in Visible Range from a Single Organic Fluorophore through Time Controlled Morphological Evolution

Ramprasad Bhatt,^a Vishal Kachwal,^b Clàudia Climent,^c Mayank Joshi,^{d,f} Pere Alemany,^c A. Roy Choudhury^f and Inamur Rahaman Laskar.^{a,*}

[a] Department of Chemistry, Birla Institute of Technology and Science, Pilani Campus, Pilani, Rajasthan 333031, India.

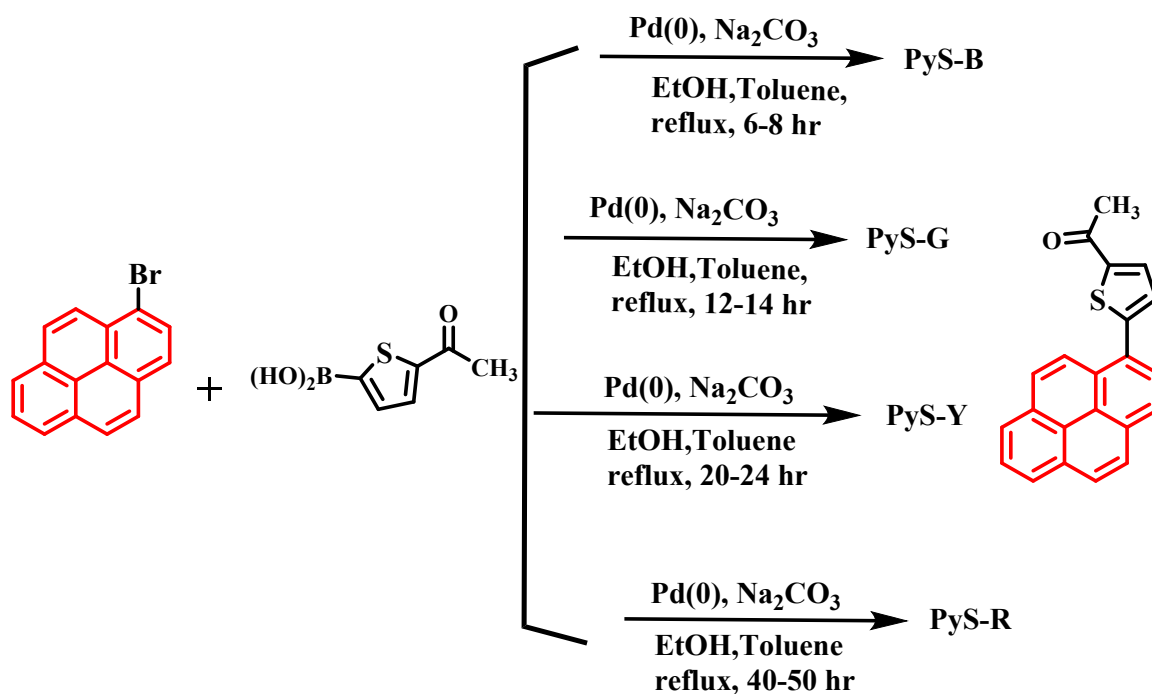
[b] Department of Engineering Science, University of Oxford, Oxford OX1 3PJ, UK.

[c] Department of Chemistry, University of Pennsylvania, Philadelphia, Pennsylvania 19104, USA.

[d] M. College of Pharmacy, Maharishi Markandeshwar Deemed to be University, Mullana, Ambala, Haryana, 133207, India.

[e] Departament de Ciència de Materials i Química Física and Institut de Química Teòrica i Computacional (IQTUB), Universitat de Barcelona, Martí i Franquès 1-11, Barcelona 08028, Spain.

[f] Department of Chemical Sciences, Indian Institute of Science Education and Research (IISER), Sector 81, S. A. S. Nagar, Manauli PO, Mohali, Punjab 140306, India.



Scheme 1. Route of synthesis of PyS

Solvents	Base	Reaction time	Temperature	Yield (%)	Product emission
Ethanol, Toluene (1:2)	1. Na ₂ CO ₃ 2. K ₂ CO ₃	6 to 50 hr	90-100 ⁰ C	60 70 86 65	Blue(6-8 hrs) Green(12-16 hrs) Yellow(20-24 hrs) Red(40-50 hrs)
1,4-dioxane	1. Na ₂ CO ₃ 2. K ₂ CO ₃	6 to 50 hr	90-100 ⁰ C	50, 65 75, 57	Blue, Green, Yellow, Red
Dimethyl formamide	1. Na ₂ CO ₃ 2. K ₂ CO ₃	6 to 50 hr	90-100 ⁰ C	55, 70 80, 55	Blue, Green, Yellow, Red

Table S1. Synthesis of PyS in the PyS-B, PyS-G, PyS-Y, and PyS-R forms at different reaction conditions.

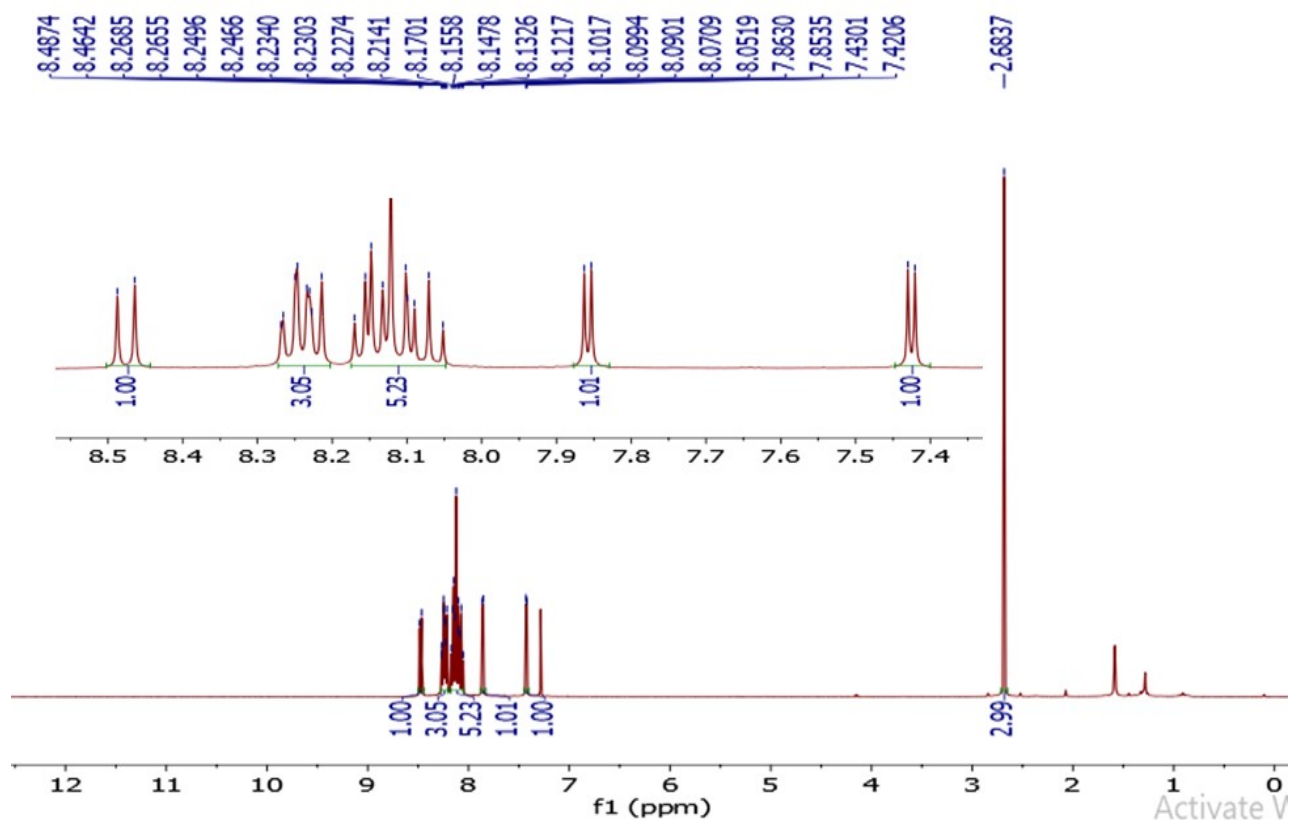


Figure S1a. ¹H NMR spectra of PyS-Y

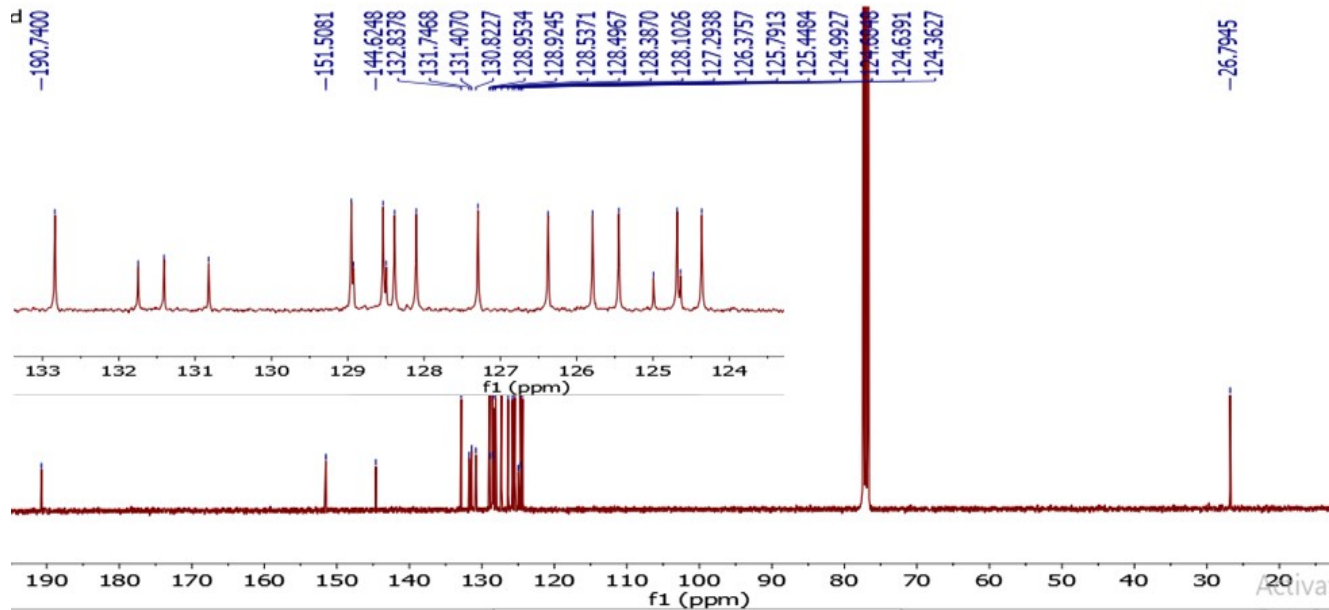


Figure S2a. ^{13}C NMR of PyS

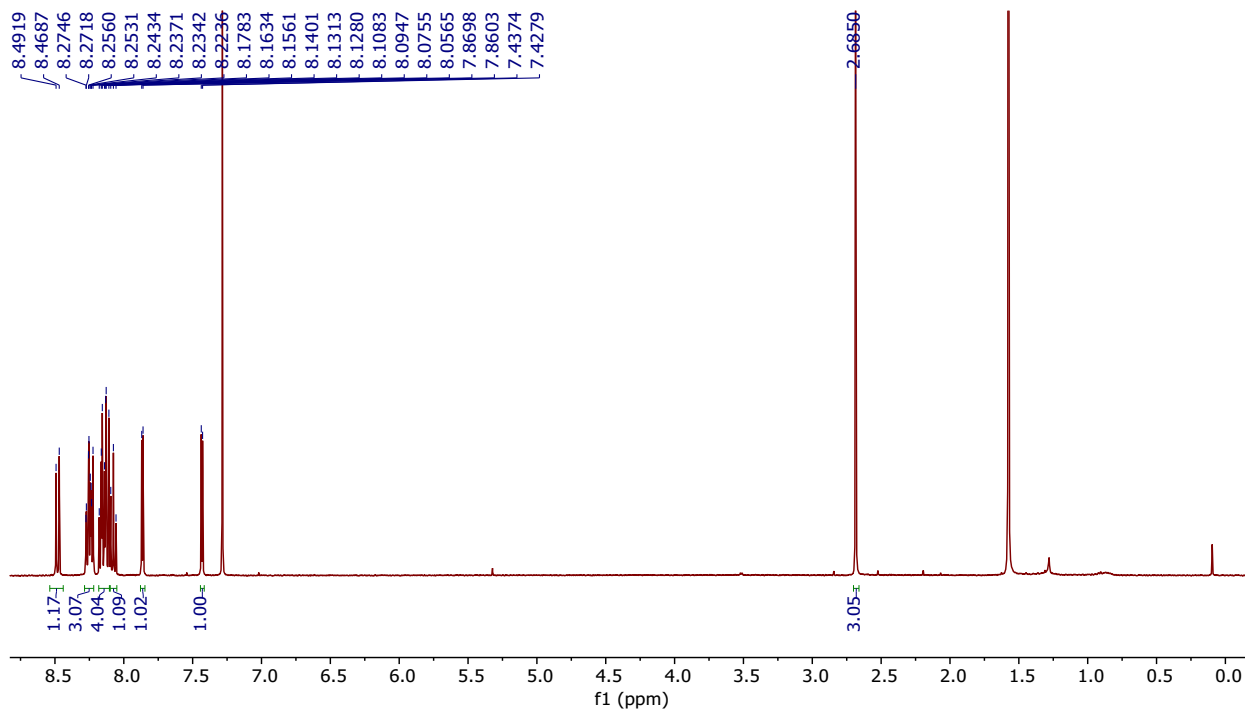


Figure S1b. ^1H NMR spectra of PyS-B

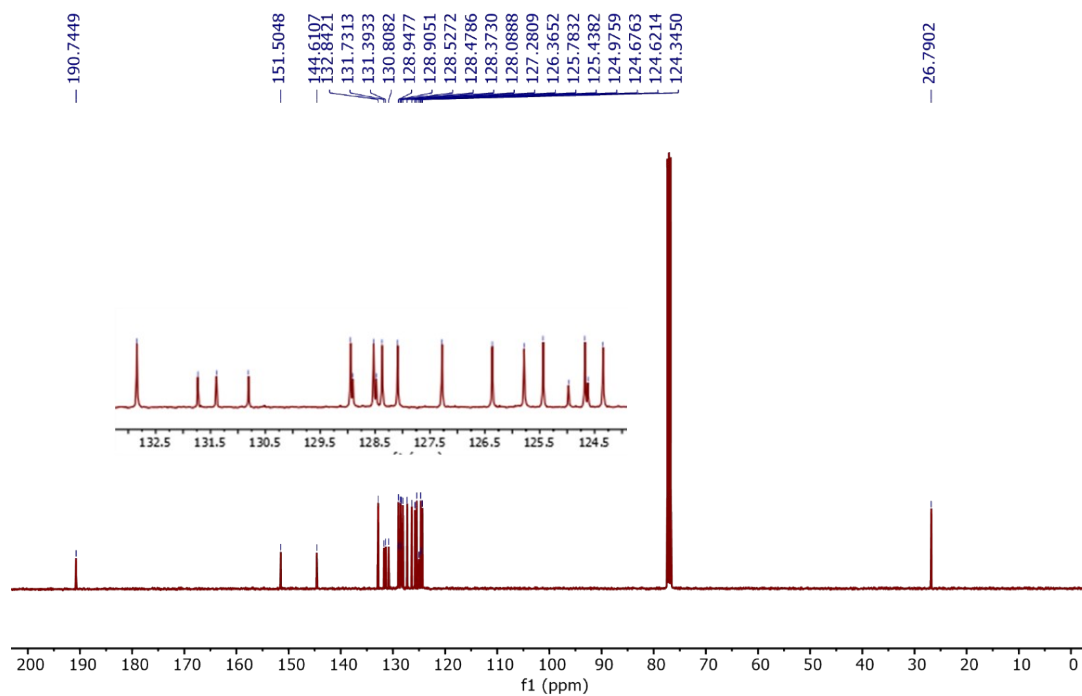


Figure S2b. ¹³C NMR spectra of PyS-B

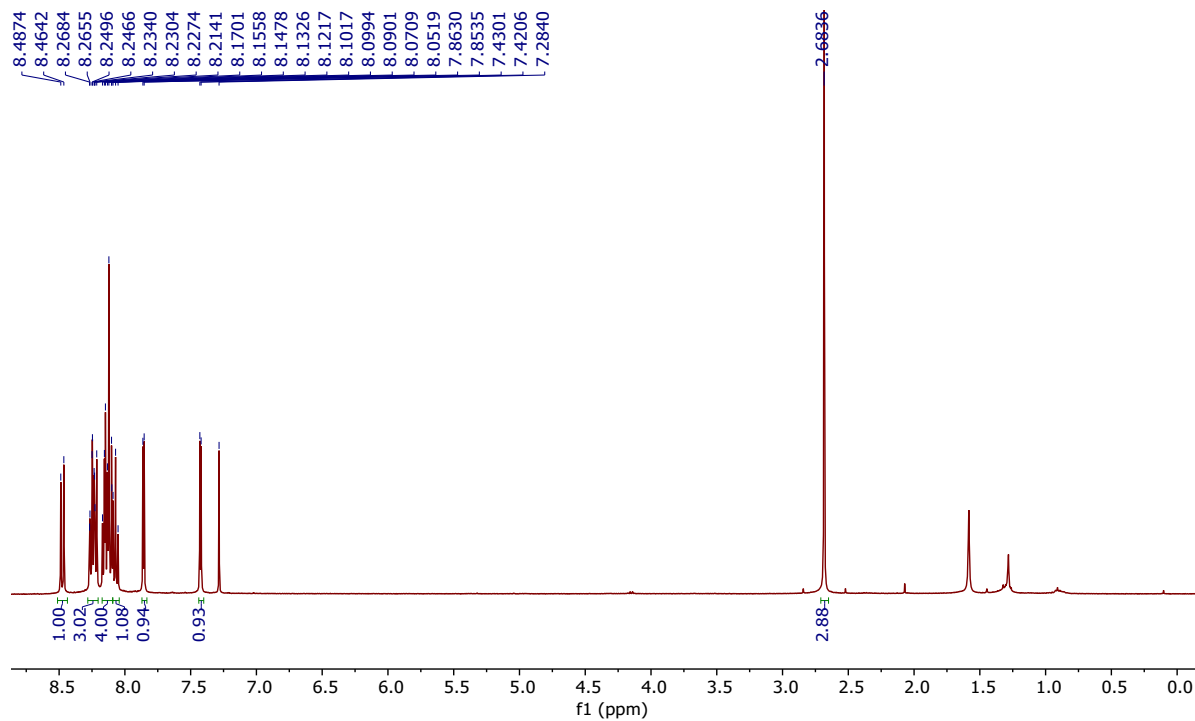


Figure S1c. ¹H NMR spectra of PyS-G

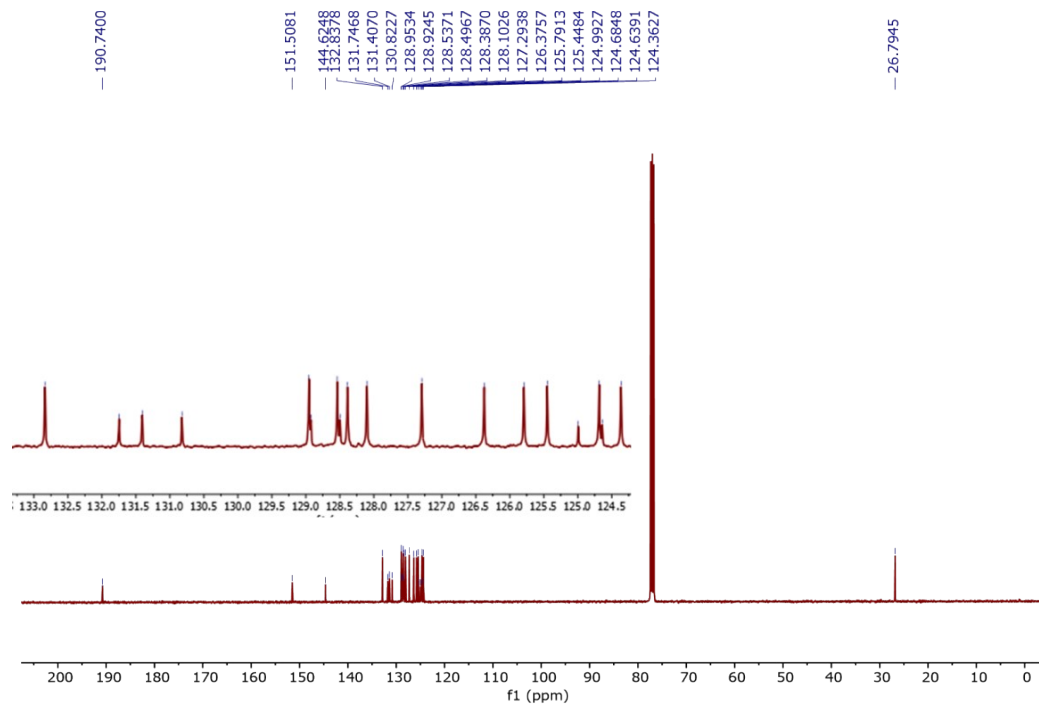


Figure S2c. ^{13}C NMR spectra of PyS-G

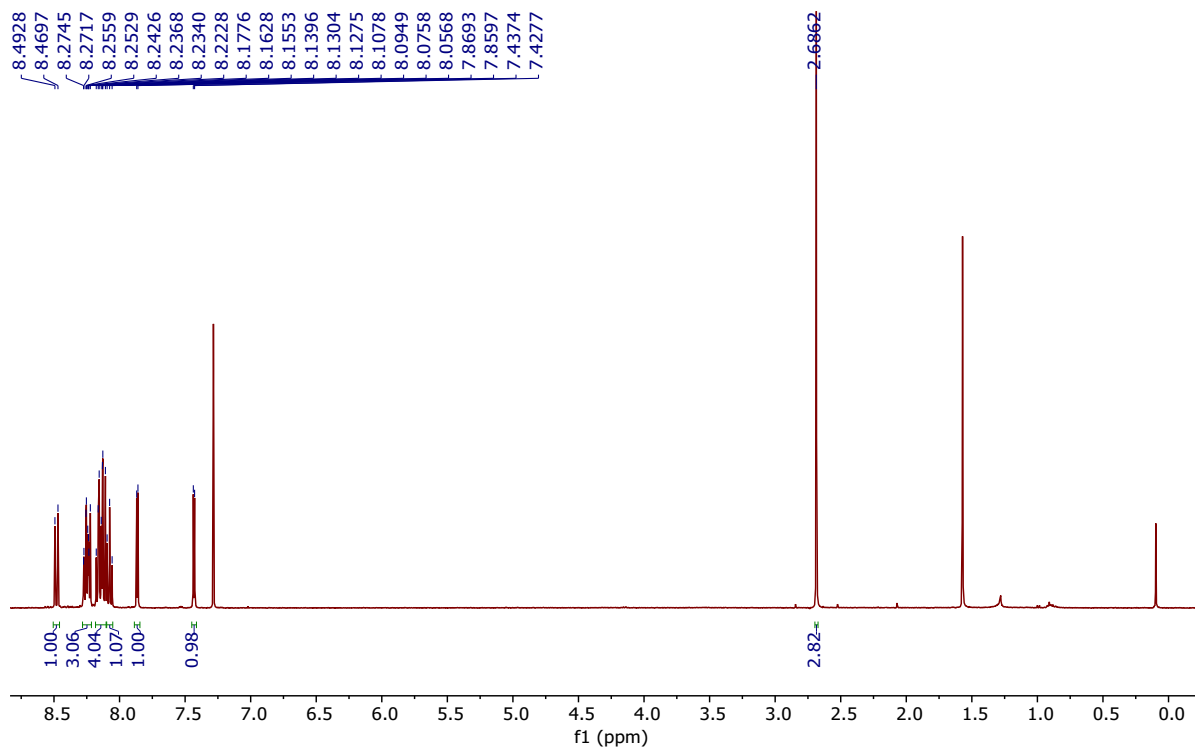


Figure S1d. ^1H NMR spectra of PyS-R

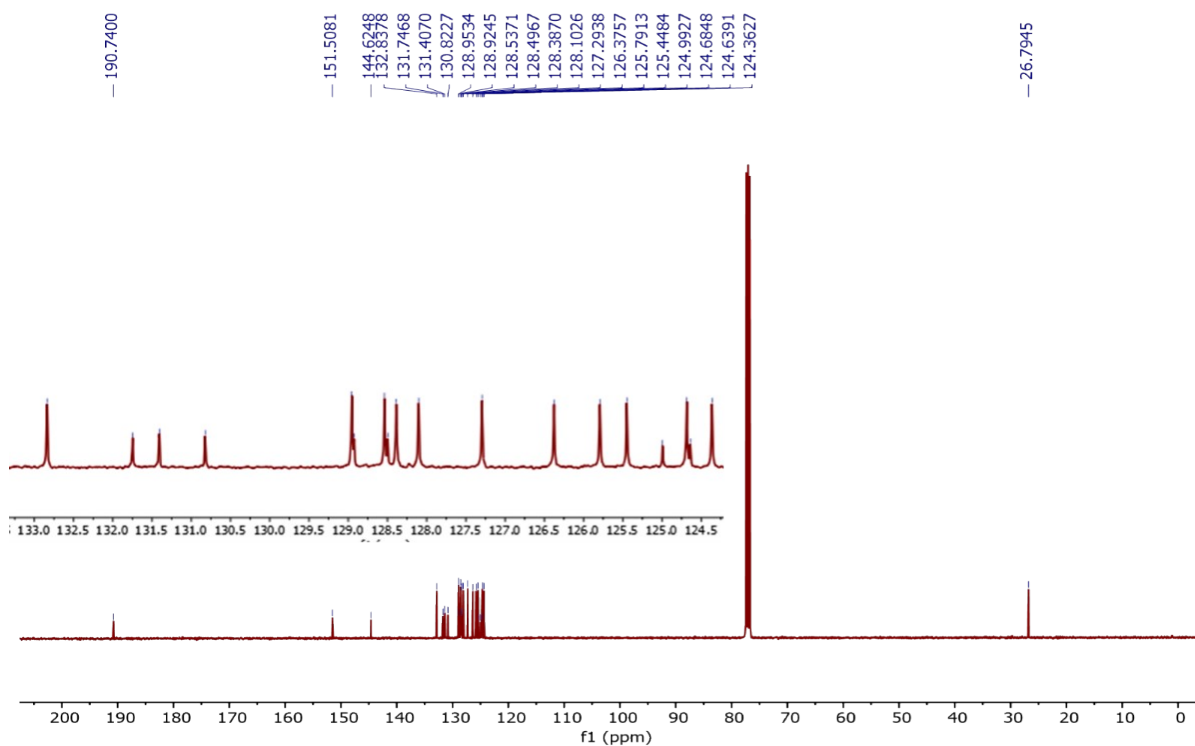


Figure S2d. ^{13}C NMR spectra of PyS-R

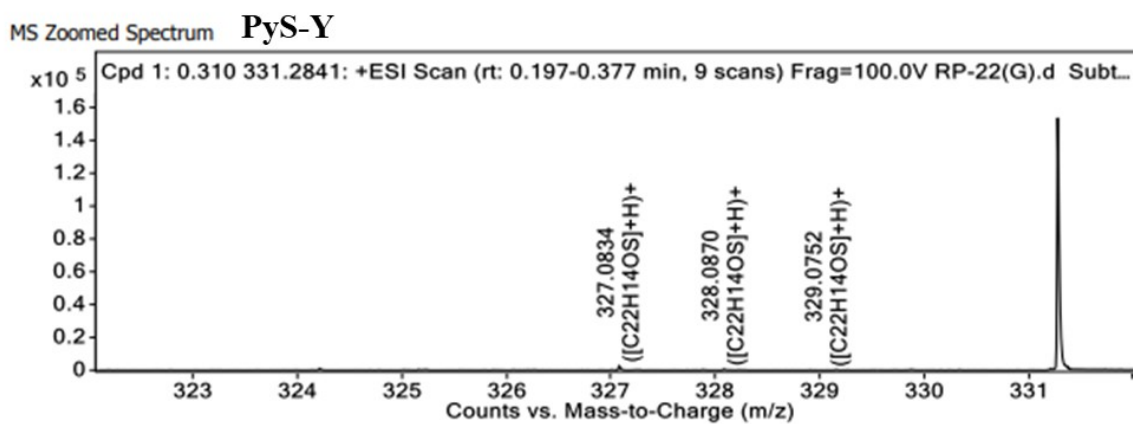
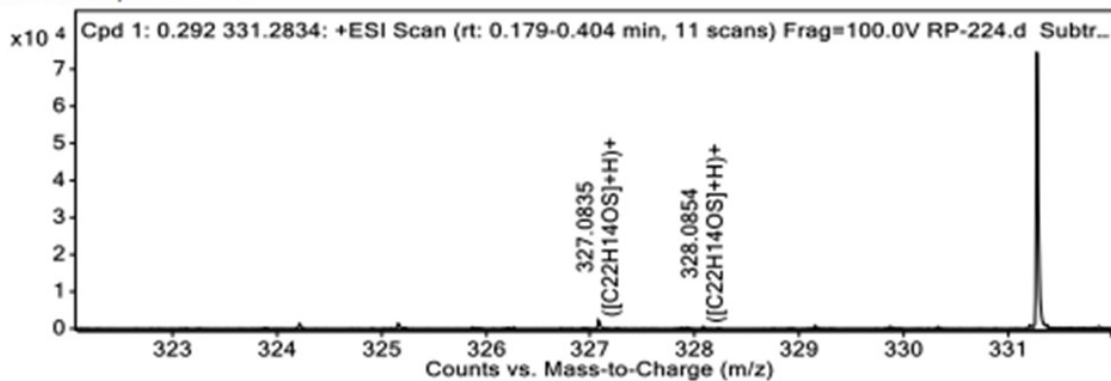
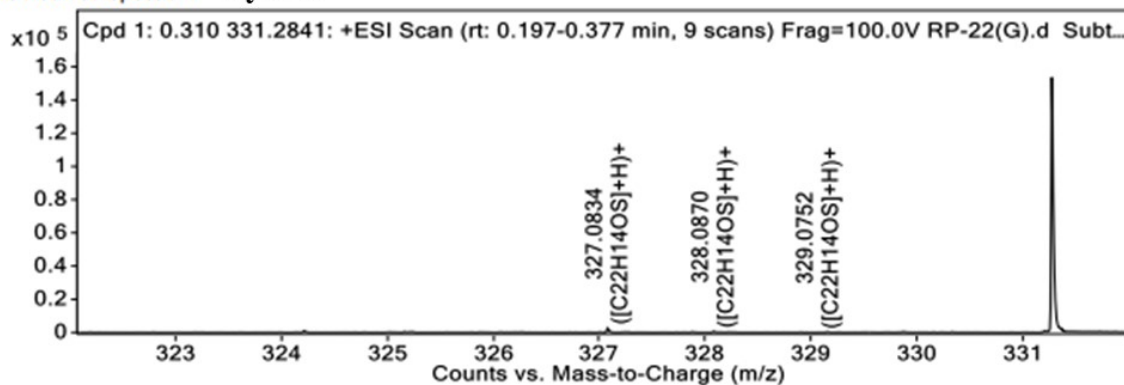


Figure S3a. HRMS data of PyS-Y, we observed m/z at 327.0837 as a major peak apart from these at same molecular formula two small peaks are observed corresponding to isotopic mass of same compound.

MS Zoomed Spectrum PyS-B



MS Zoomed Spectrum PyS-G



MS Zoomed Spectrum PyS-R

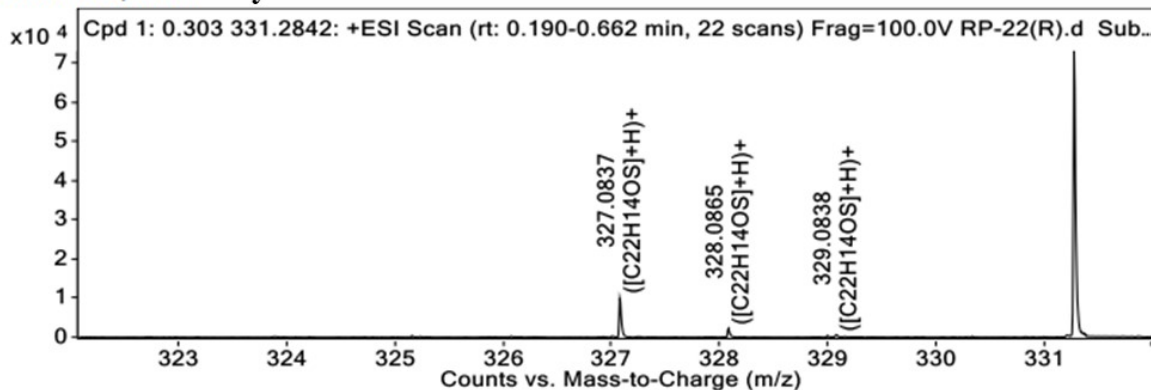


Figure S3b. HRMS data for PyS (blue, green and red emitting products). It was observed m/z at 327.0837 as a major peak apart from these at same molecular formula small peaks are observed corresponding to isotopic mass of same compounds for all three cases.

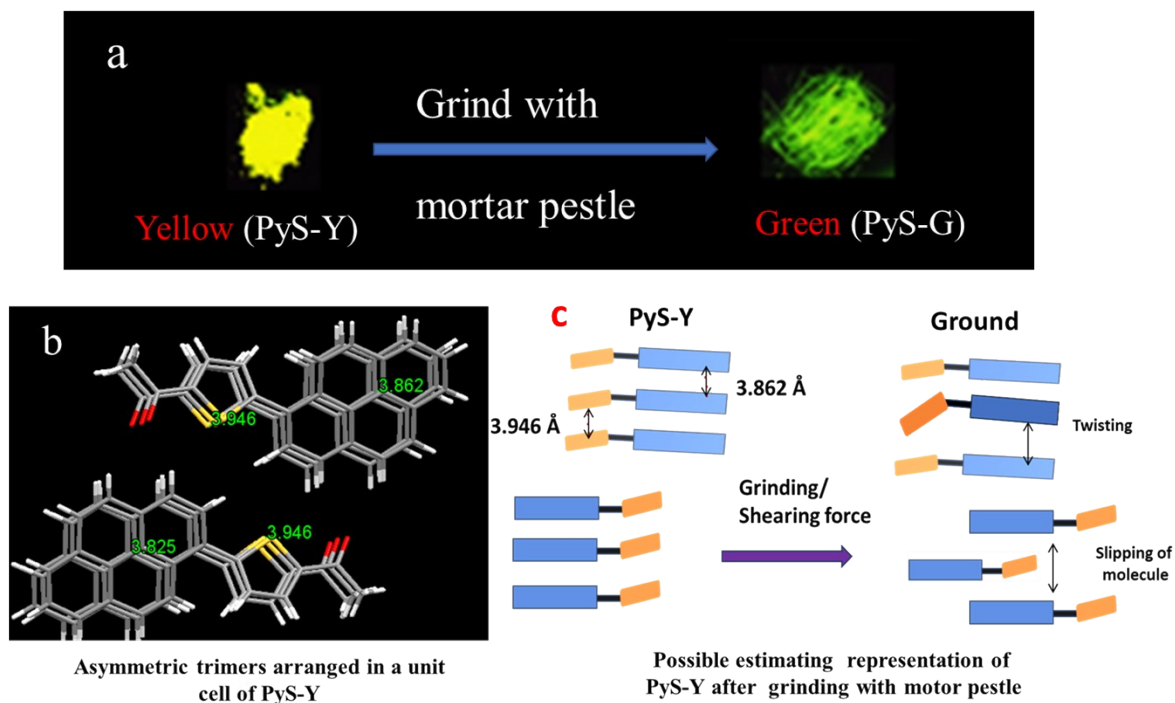


Figure S4. (a) Images of compounds taken under a UV lamp (365 nm), product of normal Suzuki coupling obtained after 24 h (PyS-Y) and ground form of PyS-Y by using mortar pestle. (b) Asymmetric trimers arranged in unit cell and (c) their possible deformation with external grinding force is shown by estimated representation to show effect of slipping and twisting.

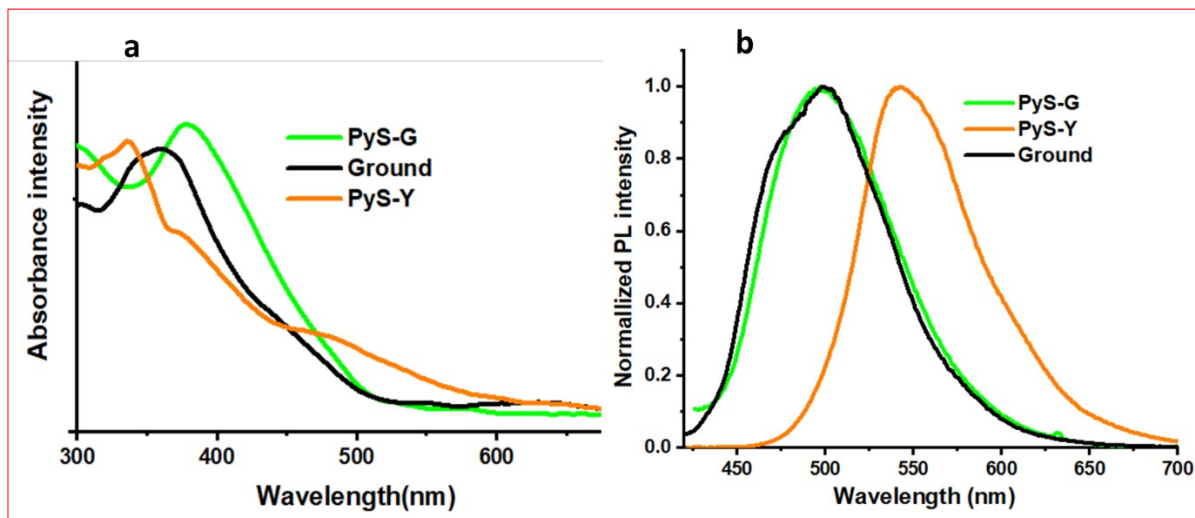


Figure S5. (a) Absorption spectra of (PyS-Y), PyS-G and ground form of PyS-Y (Ground), (b) Emission spectra of pristine powder (PyS-Y), ground form of PyS-Y (Ground) and synthesized green emissive (PyS-G).

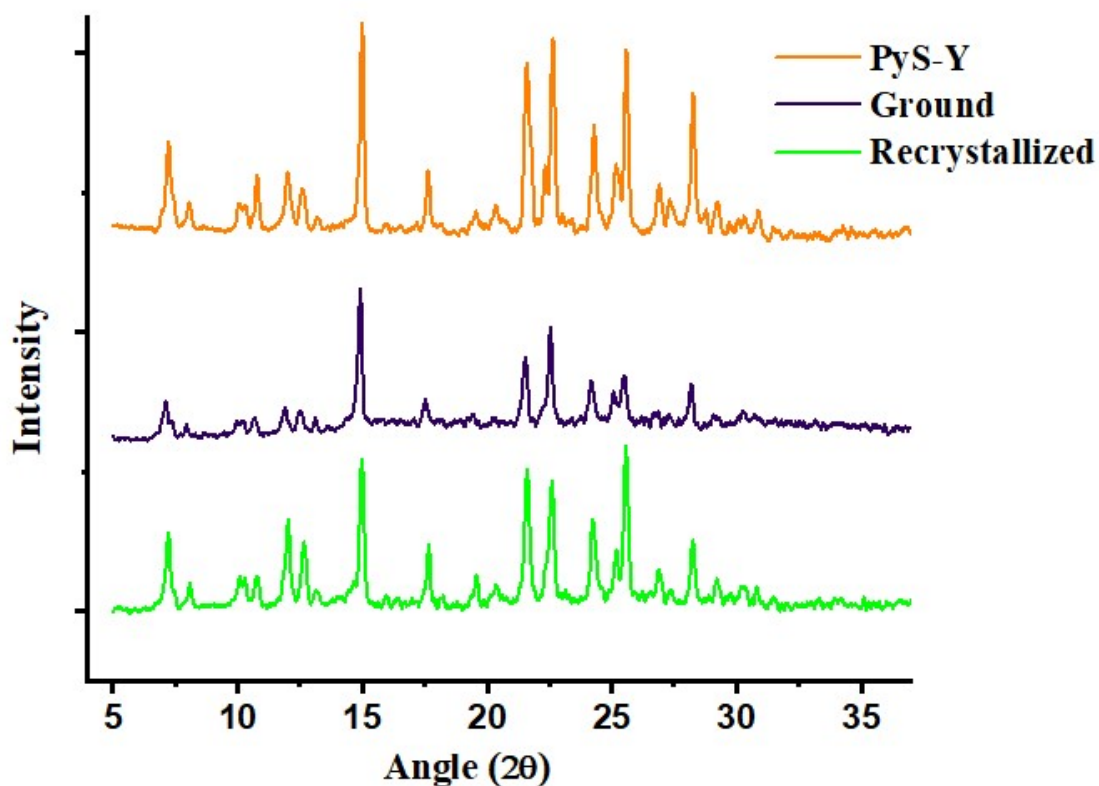


Figure S6. PXRD pattern of PyS-Y (Yellow), Ground form of PyS-Y and recrystallized form of PyS-Y in DCM, hexane.

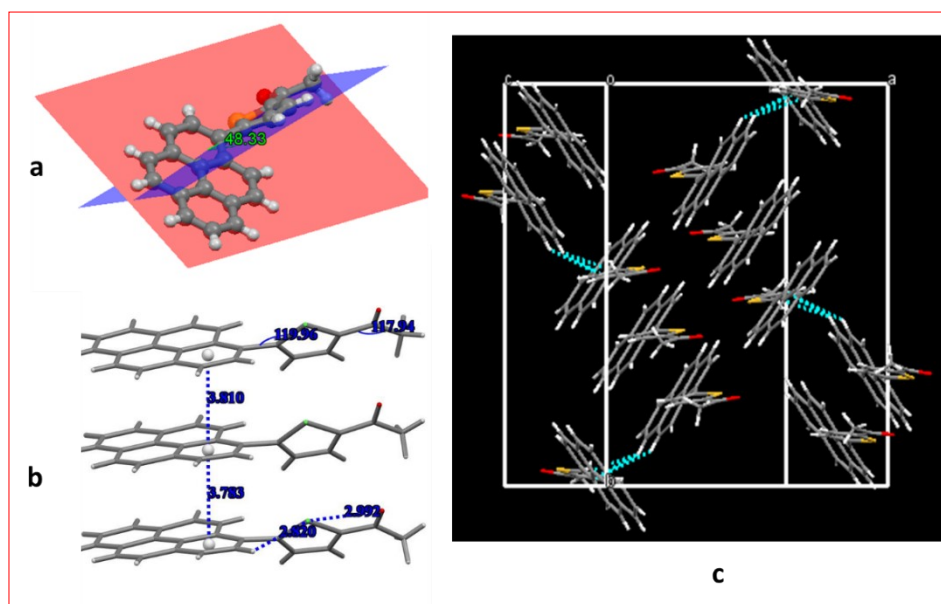


Figure S7a. Crystal structure of PyS-Y showing, (a) a single PyS molecule highlighting the dihedral angle between the pyrene and the thiophene planes (48.33°) (b) Asymmetric unit (PyS trimer) of the crystal with the separations between pyrenes planes and (c) Arrangement of the twelve molecules in the unit cell.

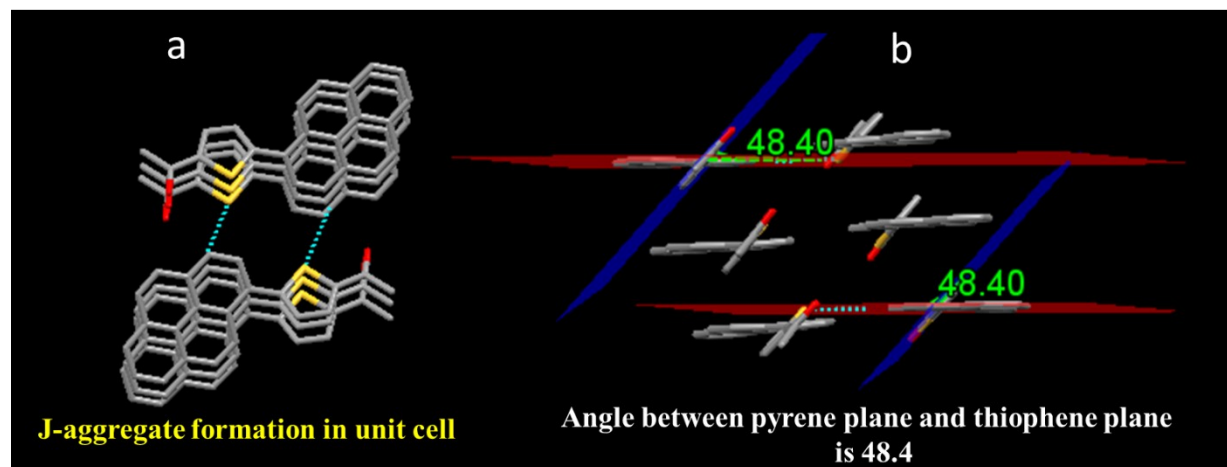


Figure S7b. (a), Asymmetric unit (PyS trimer) forming J-type arrangement with another trimer in a unit cell and (b), angle between the plane of pyrene fragments and thiophene fragments.

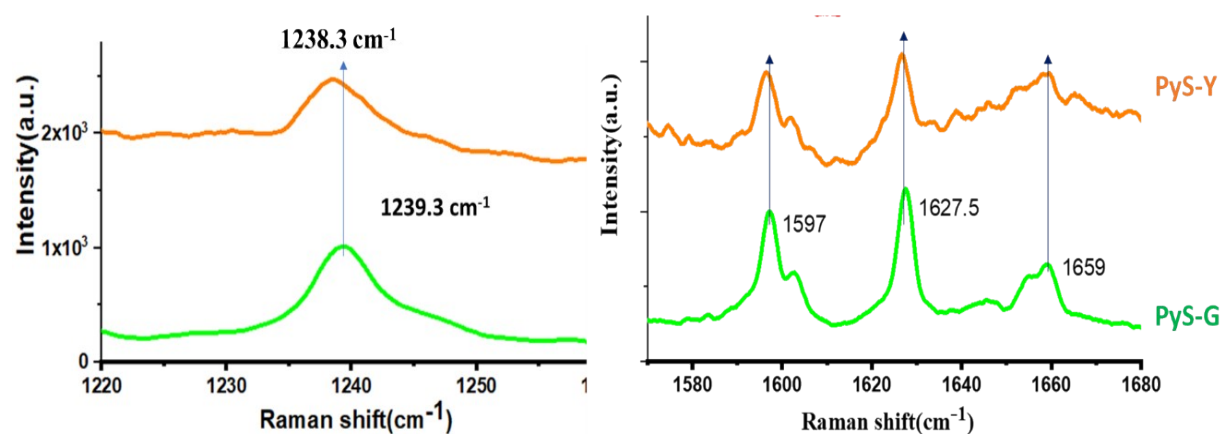


Figure S8. Raman analysis of PyS-G (ground form of PyS-Y) and PyS-Y. It was observed that the peak at 1239.3 cm⁻¹ belongs to CH in-plane bending of the pyrene ring and that the peaks at 1597 cm⁻¹ and 1627.5 cm⁻¹ correspond to the C-C stretching for pyrene. The Raman frequency at 1659 cm⁻¹ corresponds to the conjugated carbonyl C=O stretching frequency.¹

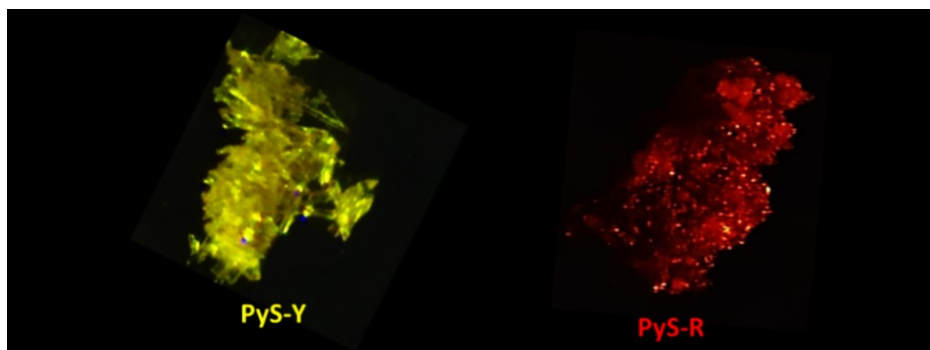


Figure S9. Fluorescence microscopic image of different coloured crystals of PyS (PyS-Y and PyS-R).

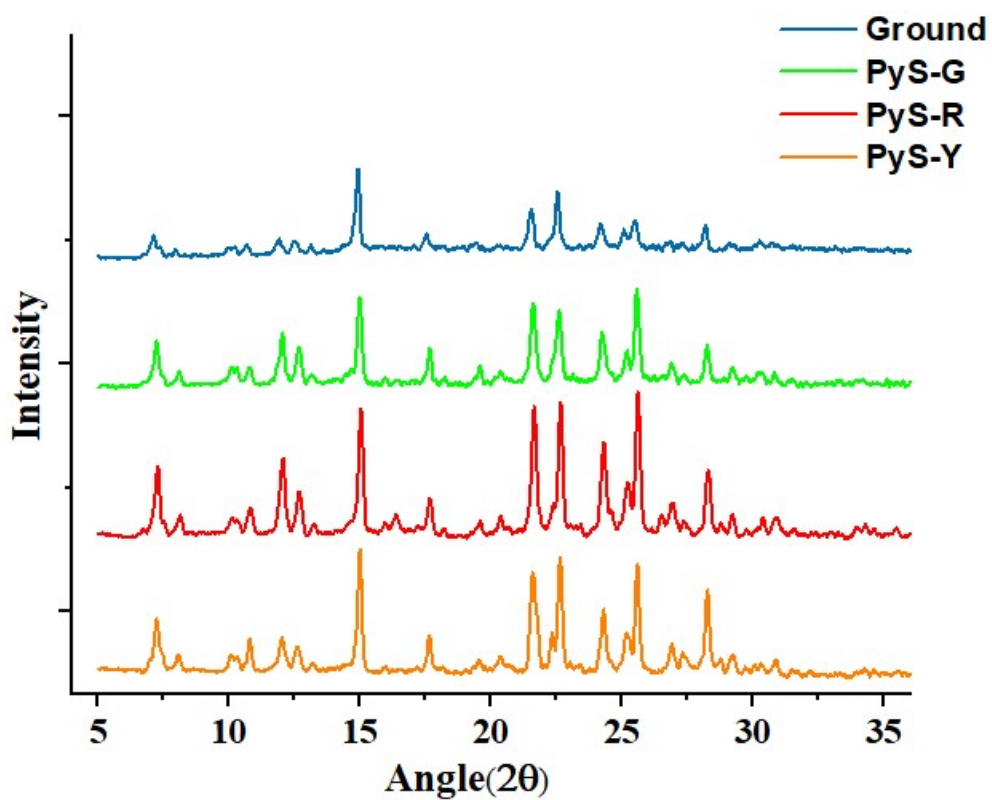


Figure S10. PXRD diagrams of PyS-B, PyS-G, PyS-Y, PyS-R samples.

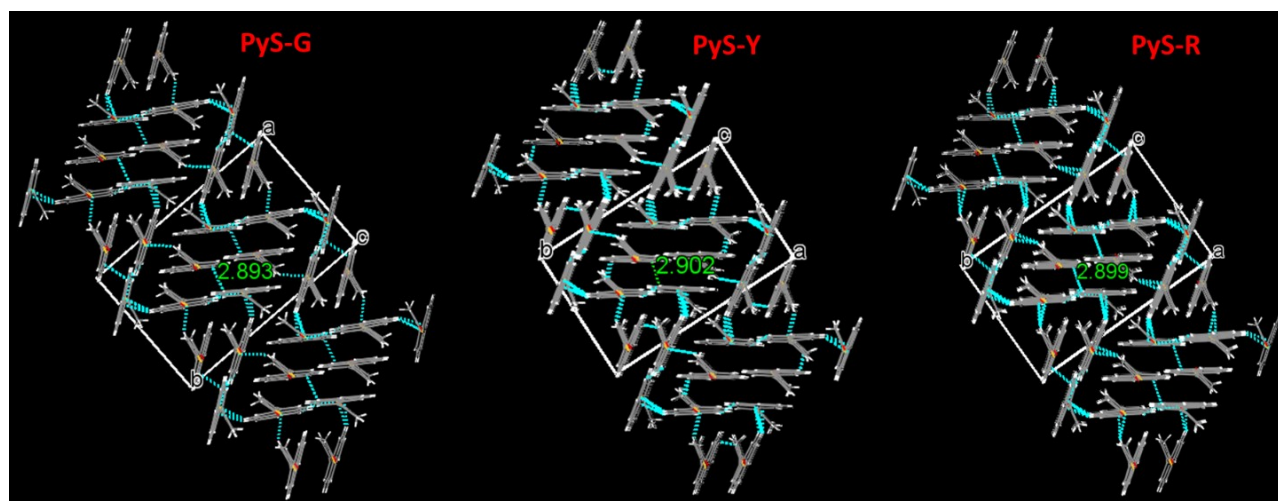


Figure S11. Crystal packing of PyS in the PyS-G, PyS-Y, and PyS-R samples and crystallographic data for PyS shown.

Crystallographic data for PyS-G, PyS-Y and PyS-R

Crystal data of PyS-G

Identification code	PyS-G
Empirical formula	C ₂₂ H ₁₄ O S
Formula weight	326.39
Temperature/K	298K
Space group	P21/n
a/Å	14.9740(5)
b/Å	21.4386(6)
c/Å	15.6550(6)
α /°	90
β /°	110.492(4)
γ /°	90
Volume/Å ³	4707.6(3)
Z	12
ρ_{calc} /cm ³	1.382
μ /mm ⁻¹	0.211
F(000)	2040.0

Crystal data of PyS-Y

Identification code	PyS-Y
Empirical formula	C ₂₂ H ₁₄ O S
Formula weight	326.39
Temperature/K	298K
Space group	P21/n
a/Å	14.989(2)
b/Å	21.458(2)
c/Å	15.650(2)
α /°	90
β /°	110.322(16)
γ /°	90
Volume/Å ³	4720.3(3)
Z	12
ρ_{calc} /cm ³	1.378
μ /mm ⁻¹	0.210
F(000)	2040.0

Crystal data of Red emitting product

Identification code	PyS-R
Empirical formula	C ₂₂ H ₁₄ O S
Formula weight	326.39
Temperature/K	298K
Space group	P21/n
a/Å	15.0076(6)
b/Å	21.4845(7)
c/Å	15.6667(6)
α /°	90
β /°	110.541(5)
γ /°	90
Volume/Å ³	4730.3(3)
Z	12
ρ_{calc} /cm ³	1.375
μ /mm ⁻¹	0.210
F(000)	2040.0

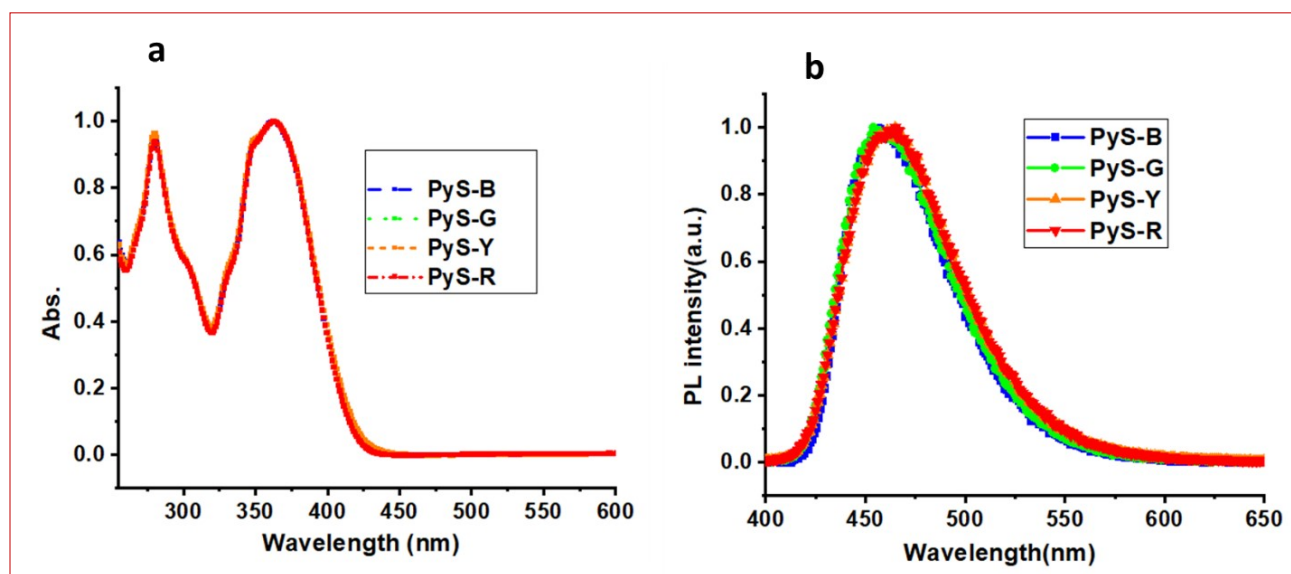


Figure S12 a) UV-visible spectra of PyS (obtained from blue, green, yellow, and red samples, respectively) in 10^{-5} M solutions of dichloromethane (b) PL spectra of the same samples in the same solution.

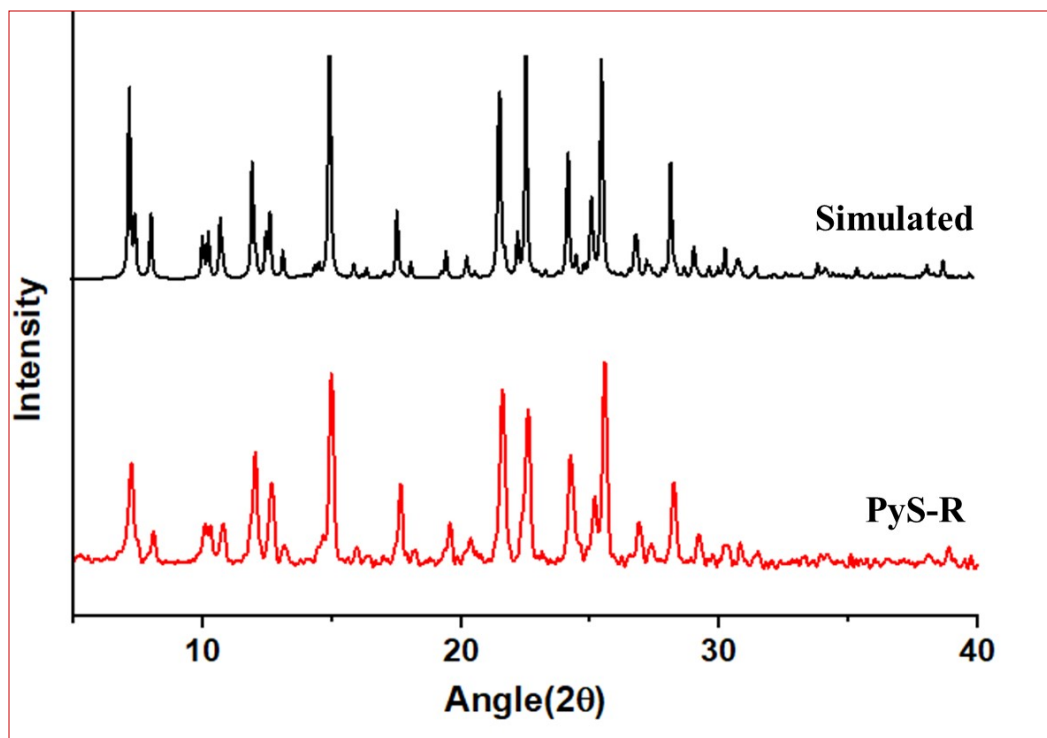


Figure S13. PXRD of PyS-R in powder and simulated form single crystal data.

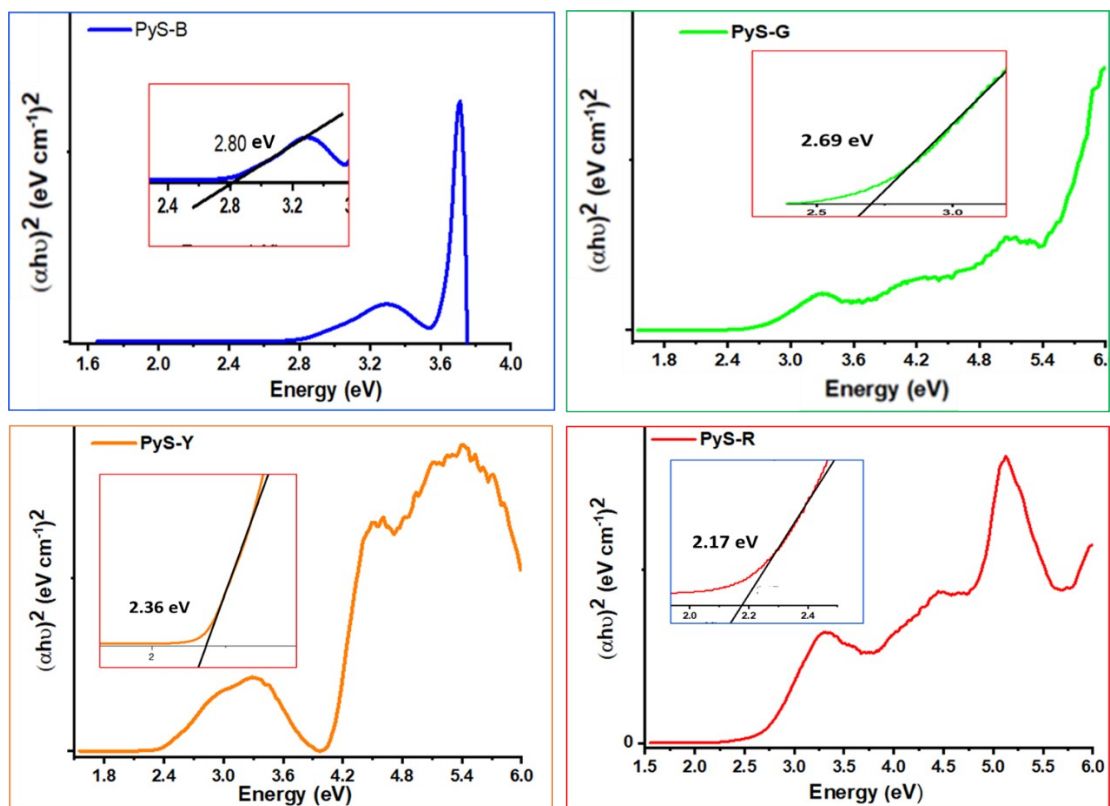


Figure S14. UV-vis DRS spectra of the all forms of PyS (PyS-B, PyS-G, PyS-Y and PyS-R) samples (inset-determination of the optical band gap).

The optical band gaps of the materials were examined by UV-vis diffuse-reflectance spectroscopy (DRS) followed by as suggested literature in ACS catalysis.² Clearly, the PyS samples increased the absorption edge moved from PyS-B to PyS-R. Then, the band gap energies (E_g values) of PyS (different color) solid were calculated using the empirical equation 1 given below.

$$(\alpha h\nu)^2 = A^2 (h\nu - E_g)^n \quad 1$$

Where, the absorption coefficient, Planck constant, light frequency, proportionality constant, and band gap energy are represented by α , h , ν , A , and E_g , respectively and $n=1$ for direct electronic transitions.

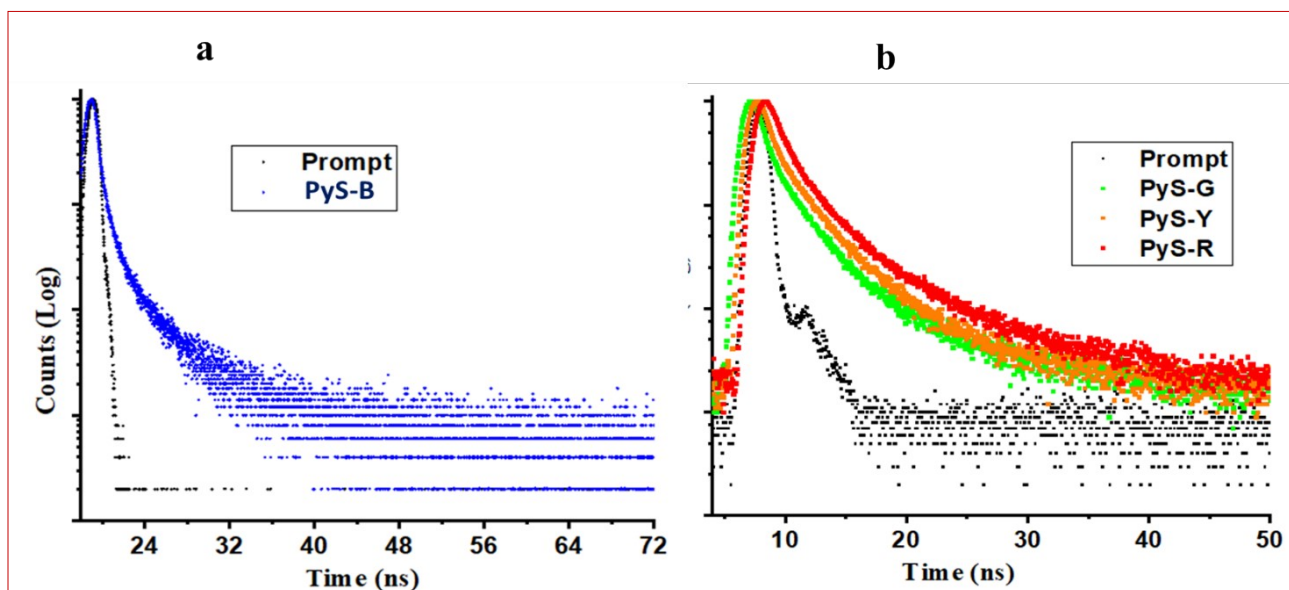


Figure S15 (a) Lifetime of PyS-B (0.6 ns) deposited on a glass coverslip and dried afterwards and (b) lifetime analysis of PyS-G (14 ns), PyS-Y (15.5 ns) and PyS-R 18.2 ns) analysed in powder form.

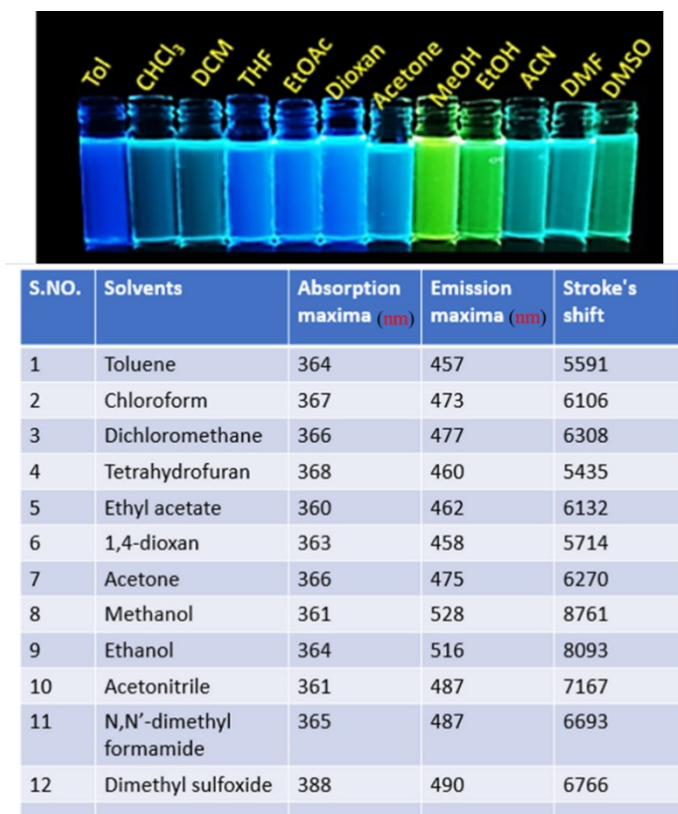


Figure S16. Optical properties of PyS solutions in different solvents, a) image of PyS with different solvents under a UV lamp (365 nm), (b) Table showing excitation and emission wavelengths and Stokes shift for each case.

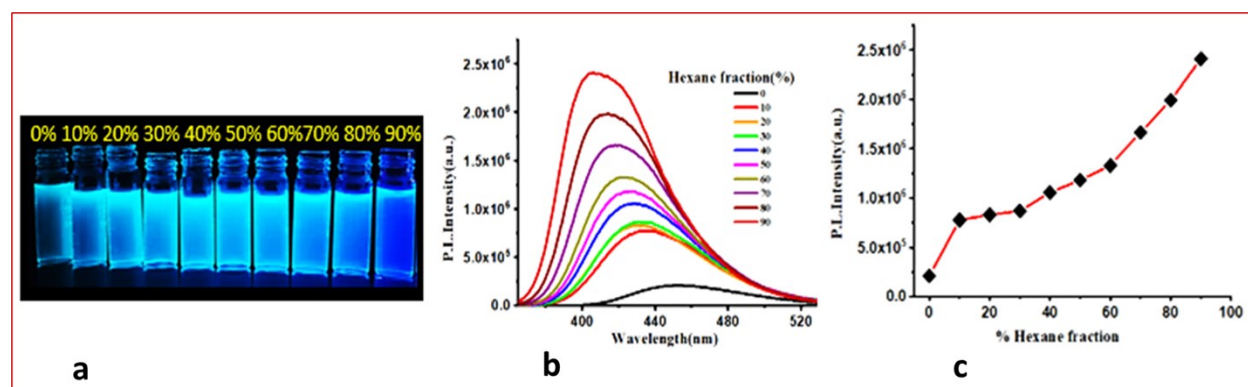


Figure S17. AEE (Aggregation-induced Enhanced Emission) active property of PyS in DCM (10^{-4} M solution) with increasing the fraction of hexane from 0 to 90 %, their image under UV lamp (365 nm) (a), PL spectra (b) and line graph for PL intensity variation with increasing hexane fraction in the solvent mixture (c).

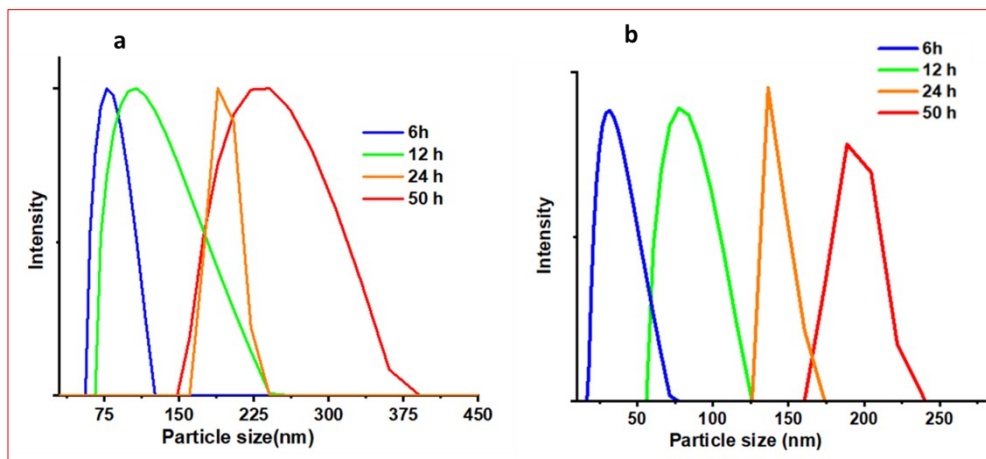


Figure S18. Particle size analysis from DLS measurement for PyS from the direct reaction mass (RM) collected at 6h, 12h, 24h and 50h time intervals and from the isolated pure products collected at the same time intervals (isolated pure compounds dissolved in Ethanol/Toluene (1:2) to record DLS)(average particle sizes found from the RM: @6h, 80 nm, @12h, 150 nm, @24h, 190 nm and @50h, 250 nm; average particle sizes from the isolated pure product:@6h, 32 nm, @15h, 82 nm, @24h, 140 nm and @50h product,- 195 nm)

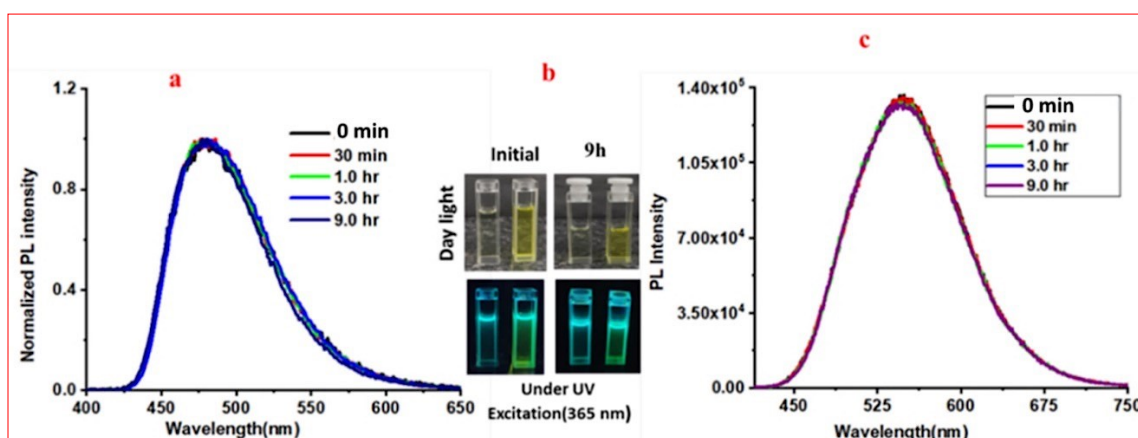


Figure S19. Fluorescence spectra of isolated pure product of PyS -G(a) and PyS-R(c) in ethanol/toluene (1:2) 10^{-3} M with time; the recorded emission spectra of the red and green species at variable time. Inset image (b) shows emission colours in daylight and Under UV excitation of 365nm for initial (0 min) and after 9 hr time.

Entry	λ_{em} (nm)	Φ_F (%)	τ_1 (ns), a (%)	τ_2 (ns), b(%)	τ_3 (ns), c(%)	$\langle \tau \rangle$ (ns)	χ^2
PyS-B	524	4.01	0.27, 55.87	0.54, 30.81	1.08, 13.32	1.0	1.16
PyS-G	583	7.9	0.48, 45.39	2.07, 35.57	5.63, 19.04	14	1.04
PyS-Y	590	11.8	0.55, 36.67	2.08, 42.93	6.59, 20.40	16	1.08
PyS-R	600	16.0	0.68, 29.54	2.09, 48.04	7.00, 22.42	18	1.18

Table S2. Solid state emission wavelength, quantum yield and excited state lifetime with components including the relative amplitude (a, b, and c in percentages) for the four different samples of PyS.

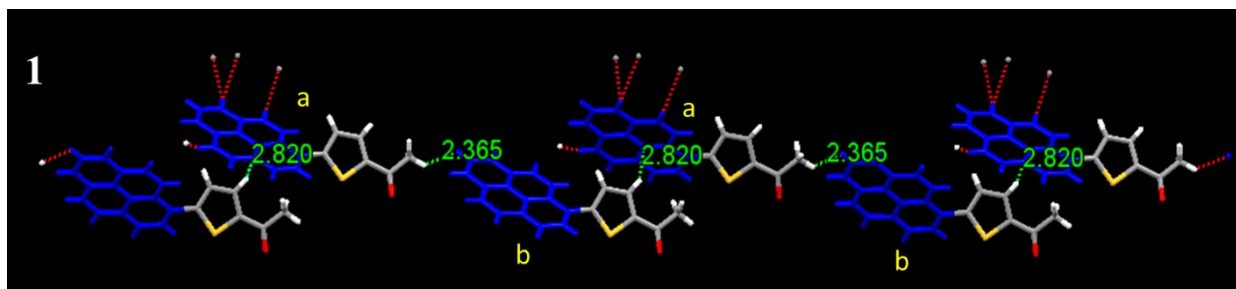


Figure S20. Crystal packing of PyS in the PyS-Y crystals, highlighting different interactions that might be involved in the morphological evolution of aggregates. In **1**, formation of chains through interaction of a thiophene ring hydrogen with pyrene π -electrons (C-H... π interactions, 2.820 Å) in a neighbouring molecule and interaction between the terminal methyl hydrogen of the acetyl group of one molecule with a hydrogen atom of the pyrene fragment (2.365 Å) of another molecule.

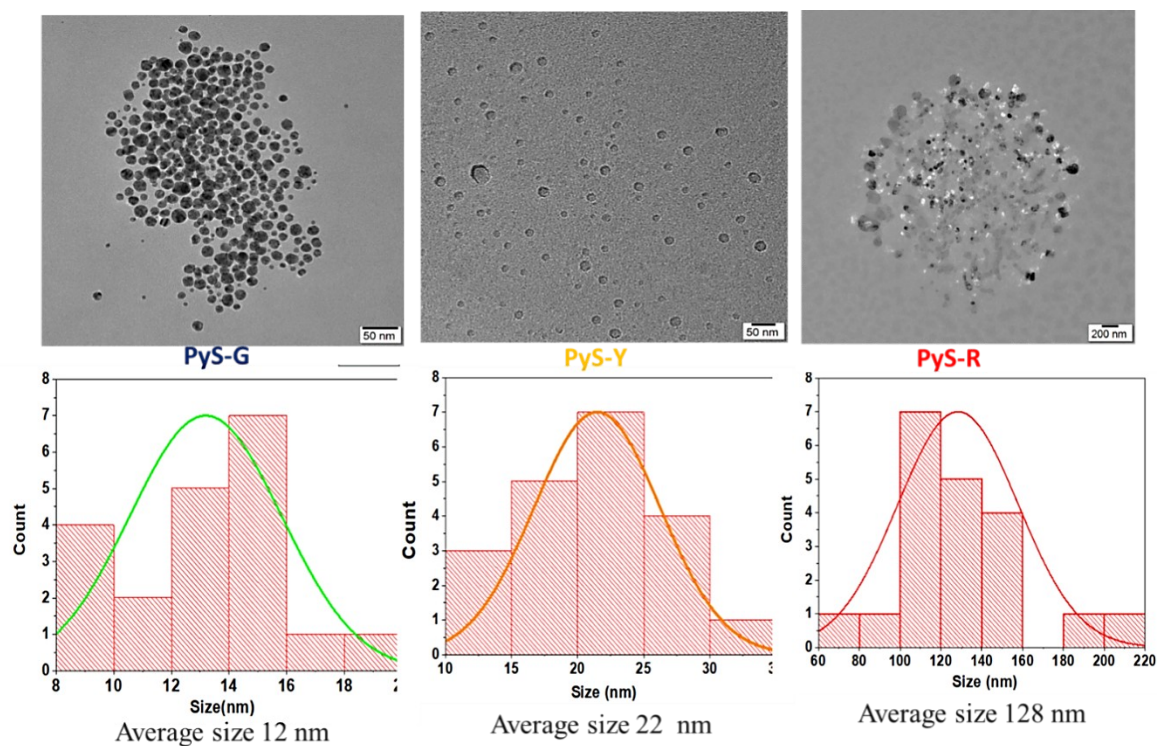


Figure S21. Average particle size and distribution from HR-TEM images of PyS-G, PyS-Y, and PyS-B samples.

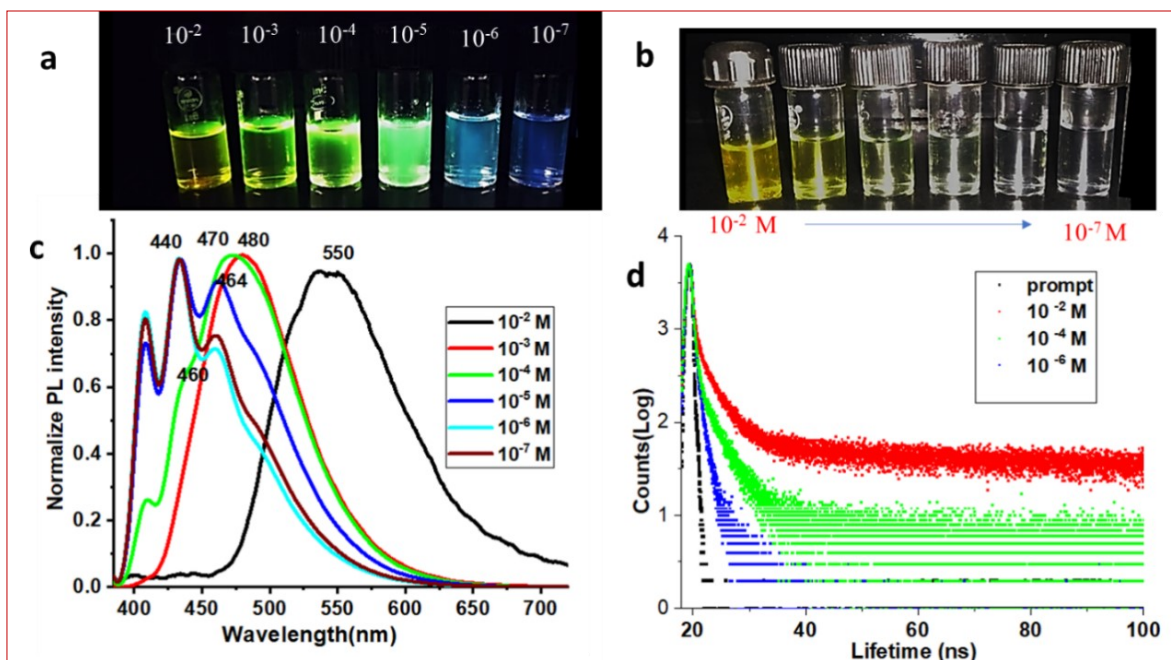


Figure S22. (a) Image of PyS-R solutions at different concentrations (from 10^{-2} M to 10^{-7} M from left to right) in toluene and ethanol (2:1) under excitation by a UV Lamp (365 nm). (b) Daylight emission of PyS-R solutions at different concentrations, (c) PL spectra of PyS-R at the same concentrations as shown in the fluorescence image in (a), (d) Lifetime measurements of PyS-R in ethanol, toluene (1:2) solution at different concentrations (10^{-2} M (5 ns), 10^{-4} M (3 ns) and 10^{-6} M (1 ns)).

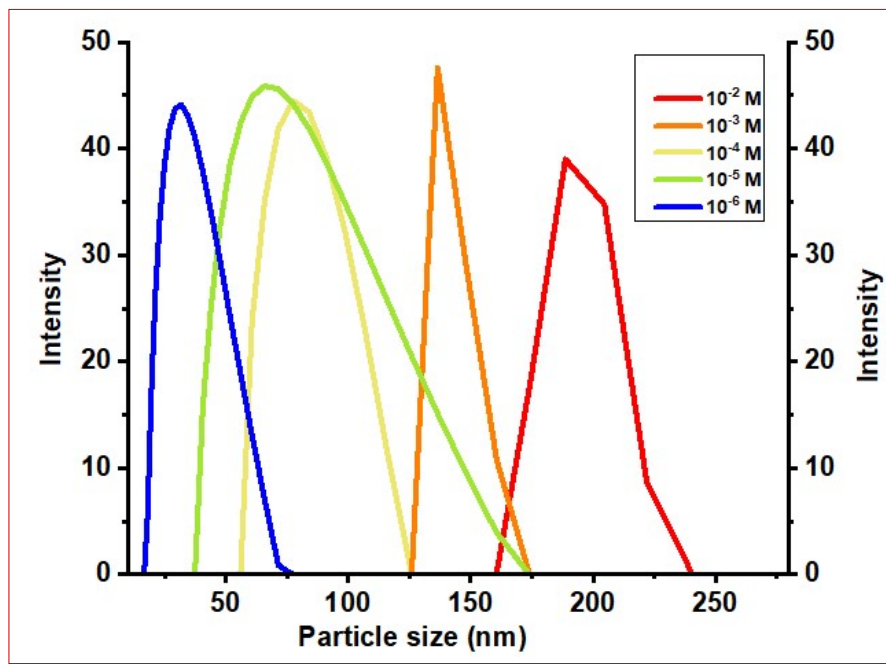
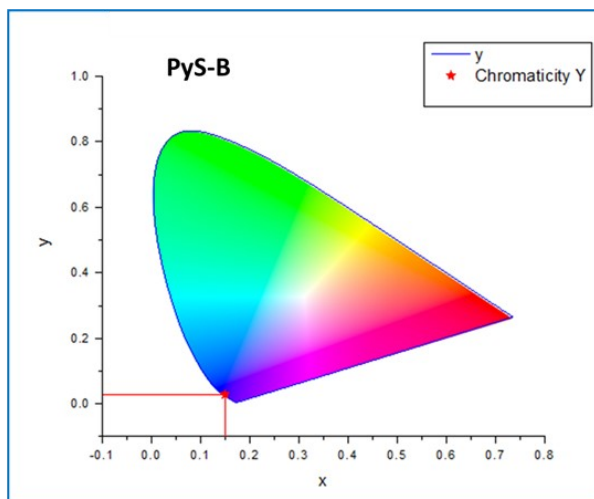
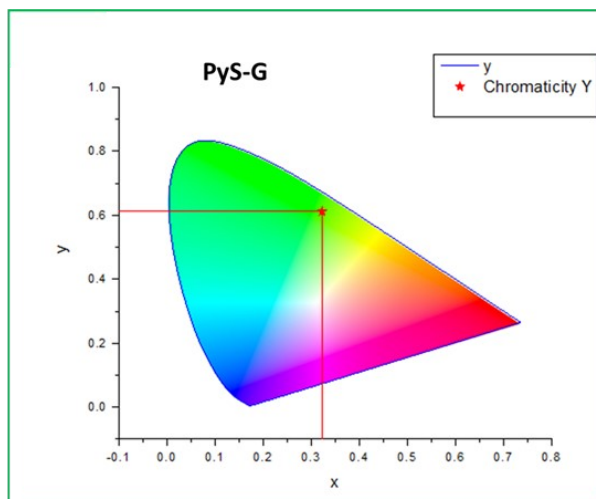


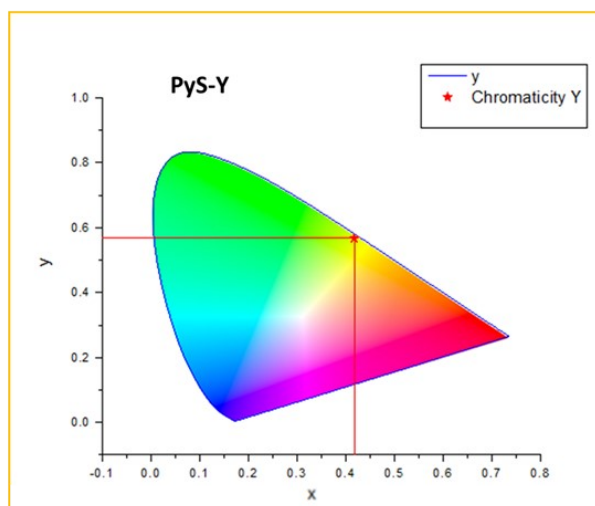
Figure S23. Particle size analysis of PyS-R in ethanol-toluene (1:2) solutions at different concentrations (10^{-2} M to 10^{-6} M).



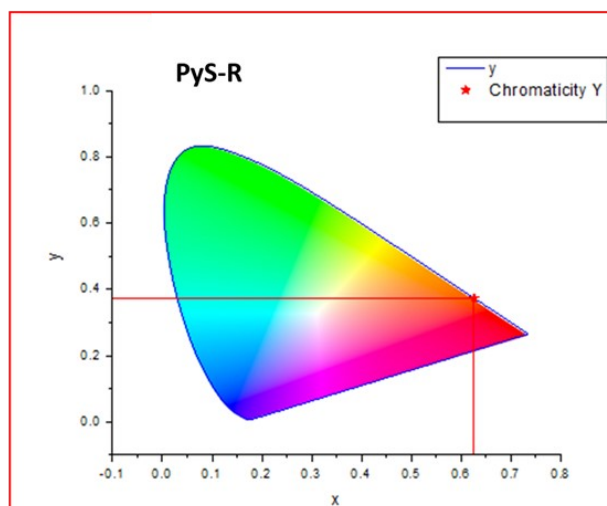
Color coordinates - (0.1497, 0.0293)



Color coordinates - (0.3224, 0.6119)



Color coordinates - (0.4172, 0.5674)



Color coordinates - (0.6262, 0.3734)

Figure S24. CIE colour coordinates of PyS-B, PyS-G, PyS-Y, and PyS-R.

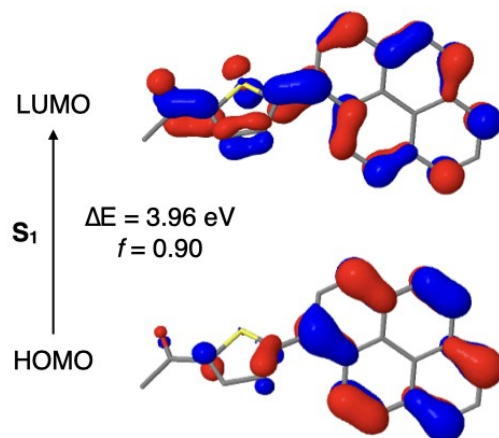


Figure S25. Frontier molecular orbitals responsible for the S_1 excited state of the lowest-energy conformer of the PyS molecule.

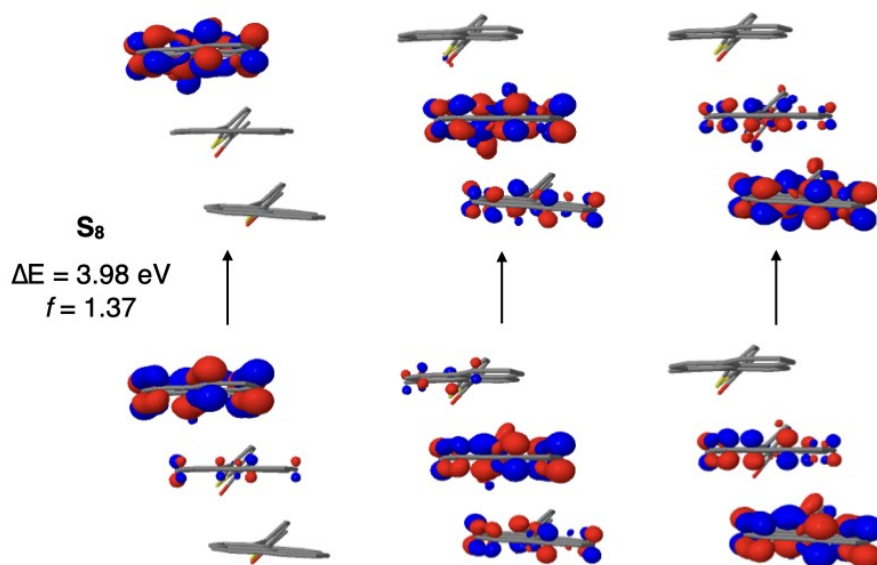


Figure S26. Main occupied-to-virtual molecular orbital contributions responsible for the brightest lowest-energy singlet excited state of the PyS trimer from the experimental crystal structure.

Computational details

All electronic structure calculations were performed with the Gaussian package.³ The structure and relative energies of the four possible conformers and the interconversion barriers were evaluated using the M062x functional⁴ with the Def2TZVP basis set.⁵ As it is well known, it is necessary to include a long-range correction for exchange functionals to solve the underestimations of charge transfer excitation energies and oscillator strengths in time-dependent Kohn–Sham calculations⁶. For this reason, excited state calculations were performed using time-dependent density functional

theory calculations within the Tamm-Dancoff approximation (TDA) with the ω B97X-D exchange-correlation functional⁷ and the 6-31G(d) basis set.

Crystallographic Details

Single crystal X-ray diffraction data was collected on Rigaku XtaLABmini X-ray diffractometer equipped with Mercury CCD detector with graphite monochromatic Mo-K α radiation ($\lambda = 0.71073 \text{ \AA}$) at 100.0 (2) K using ω scans. The data was reduced using CrysAlisPro 41_64.93a software.⁸ The crystal structures were solved using Olex² package⁹ equipped with XT¹⁰ and were further refined using XL.¹¹ Crystal packing and interaction diagrams were created using Mercury.¹²

1. Y. Xie, X. Wang, X. Han, X. Xue, W. Ji, Z. Qi, J. Liu, B. Zhao and Y. Ozaki, *Analyst*, 2010, **135**, 1389-1394.
2. 2. Xu, C.; Huang, W.; Li, Z.; Deng, B.; Zhang, Y.; Ni, M.; Cen, K., *ACS catalysis* **2018**, *8* (7), 6582-6593.
3. Gaussian 16, Revision C.01, M. J. Frisch, G. W. Trucks, H. B. Schlegel, G. E. Scuseria, M. A. Robb, J. R. Cheeseman, G. Scalmani, V. Barone, G. A. Petersson, H. Nakatsuji, X. Li, M. Caricato, A. V. Marenich, J. Bloino, B. G. Janesko, R. Gomperts, B. Mennucci, H. P. Hratchian, J. V. Ortiz, A. F. Izmaylov, J. L. Sonnenberg, D. Williams-Young, F. Ding, F. Lipparini, F. Egidi, J. Goings, B. Peng, A. Petrone, T. Henderson, D. Ranasinghe, V. G. Zakrzewski, J. Gao, N. Rega, G. Zheng, W. Liang, M. Hada, M. Ehara, K. Toyota, R. Fukuda, J. Hasegawa, M. Ishida, T. Nakajima, Y. Honda, O. Kitao, H. Nakai, T. Vreven, K. Throssell, J. A. Montgomery, Jr., J. E. Peralta, F. Ogliaro, M. J. Bearpark, J. J. Heyd, E. N. Brothers, K. N. Kudin, V. N. Staroverov, T. A. Keith, R. Kobayashi, J. Normand, K. Raghavachari, A. P. Rendell, J. C. Burant, S. S. Iyengar, J. Tomasi, M. Cossi, J. M. Millam, M. Klene, C. Adamo, R. Cammi, J. W. Ochterski, R. L. Martin, K. Morokuma, O. Farkas, J. B. Foresman, and D. J. Fox, Gaussian, Inc., Wallingford CT, 2016.
4. Y. Zhao, , D.G. Truhlar, *Theor Chem Account*, 2008, **120**, 215–241.
5. F. Weigend, R. Ahlrichs, *Phys. Chem. Chem. Phys.*, 2005, **7**, 3297-305.
6. T. Tsuneda, K. Hirao, *WIREs Comput. Mol. Sci.* 2014, 4:375–390. doi: 10.1002/wcms.1178
7. J.-D. Chai, M. Head-Gordon, *Phys. Chem. Chem. Phys.* 2008, **10**, 6615–6620.
8. CrysAlisPRO. Oxford Diffraction /Agilent Technologies UK Ltd, Yarnton, England.
9. Dolomanov, O. V.; Bourhis, L. J.; Gildea, R. J.; Howard, J. A. K.; Puschmann, H. OLEX2: A Complete Structure Solution, Refinement and Analysis Program. *J. Appl. Crystallogr.* 2009, **42**, 339–341.
10. Sheldrick, G. M. Crystal Structure Refinement with SHELXL. *Acta Crystallogr. Sect. C Struct. Chem.* 2015, **71**, 3–8.
11. Sheldrick, G. M. A Short History of SHELX. *Acta Crystallographica Section A: Foundations of Crystallography*. International Union of Crystallography January 1, 2008, 112–122.
12. Macrae, C. F.; Bruno, I. J.; Chisholm, J. A.; Edgington, P. R.; McCabe, P.; Pidcock, E.; Rodriguez-Monge, L.; Taylor, R.; Van De Streek, J.; Wood, P. A. Mercury CSD 2.0 - New Features for the Visualization and Investigation of Crystal Structures. *Journal of Applied Crystallography*. International Union of Crystallography April 1, 2008, 466–470.